INTERNATIONAL JOURNAL OF
COASTAL & OFFSHORE ENGINEERING
IJCOE Vol.7/No. 1/Winter 2022 (23-33)

Available online at: www.ijcoe.org

Semi-active Control of an Offshore Platform Using Updated Numerical Model and Experimental Laser Doppler Vibrometer Data

Samira Mohammadyzadeh[1], Alireza Mojtahedi[2*], Javad Katebi[3], Hamid Hokmabady[4], Farhad Hosseinlou[5]

[1]School of Engineering, University of Northern British Columbia, Prince George, Canada. mohammady@unbc.ca
[2]Associated Professor, Department of Water Resources Engineering, University of Tabriz, Iran. a.mojtahed@tabrizu.ac.ir*
[3]Associated Professor, Department of Structural Engineering, University of Tabriz, Iran, jkatebi@tabrizu.ac.ir
[4]Postdoctoral Research Assistant, Department of Water Resources Engineering, University of Tabriz, Iran. h.hokmabady@tabrizu.ac.ir
[5]Assistant Professor, Faculty of civil engineering and architecture, Shahid Chamran University of Ahvaz, Iran.

ARTICLE INFO

Article History:
Received: 07 Jul. 2021
Accepted: 15 Dec. 2022

Keywords:
Numerical Model Updating
Laser Doppler Vibrometer
Offshore Structure
Semi-active Control
MR damper

ABSTRACT

In this study, a semi-active control system is assessed over a numerically updated model to achieve the most promising numerical results and to keep the performance of the numerical model as close to the prototype behavior as possible. Numerical model updating is performed based on the experimentally captured non-contact sensing data considering uncertainties. The elastic modulus of the jacket elements is specified as the calibration parameter. A mathematical function -optimized using Particle Swarm Optimization (PSO) algorithm- is also employed to reduce the structural uncertainties of the numerical model. Eight MR dampers both in X and Y directions are located in a platform numerical model. Modified Newmark-Beta method besides optimized parameters of instantaneous optimal control algorithm are utilized to predict the response of the system. The performance of the updated model is evaluated under environmental loads. The results indicate the importance of model uncertainty reduction in improving the accuracy of simulation results in a complex system. Based on the results using a non-contact sensing technology such as Laser Doppler Vibrometer (LDV) system is strongly recommended in practical cases due to great sensitivity capabilities and also no direct contact requirements.

1. Introduction

Environmental loads in offshore area may cause continuous vibrations that results in decrement of reliability, productivity, and serviceability of the structures and also increment in uncertainties and possibility of the damage and failures. However, controlling the vibrations in marine structures is challenging due to nonlinear hydrodynamic forces, uncertainties, large deformations, and highly nonlinear responses [1]. Basically, vibration control methods are classified as passive, active, semi-active, and hybrid methods, each of which is widely discussed in the literature [2-7]. Semi-active control systems show higher reliability and more efficient control effects [2]. Among different semi-active control devices, Magnetorheological (MR) damper used in this study, represented a great control performance based on previous studies [8-10]. MR fluids change from a free-flowing, linear viscous liquid into semi-solid fluid in the presence of a magnetic field. A range of researches has been performed due to the capability of MR dampers in offshore structures in the literature [11-12]. A semi-active control method might be affected by the presence of uncertainties. Simply put, many factors in experimental and numerical simulation processes in any engineering fields specifically offshore structures can cause uncertainties in which their identification are of great importance [13]. Offshore environment related uncertainties can be categorized into: aleatory (natural) uncertainties and epistemic (knowledge-based) uncertainties. Aleatory uncertainty presents a quantity natural randomness, which cannot be decreased or eliminated such as time dependent wave height variability. In the other hand, epistemic uncertainty, which is related to reducible errors that can be reduced by collecting more information about a quantity, e.g. data, statistical, model and climatic uncertainties, [14]. Uncertainty quantification in both the data and the behavior prediction of models are important and must be mathematically understood to perform correctly for calibration and validation processes [13]. Complex

engineering systems response prediction needs advanced computer simulations and experimental evidence which basically requires theoretical foundation, numerical modeling, and experimental data, all of which come with their associated errors [15]. An essential rule in validating the study results is to compare the computer model predictions results to experimental data. Uncertainty reduction method is carried out by: (i) calibrating some numerical parameters through numerical model updating used for reproducing the experimental data or (ii) by changing some experimental parameters to reproduce the numerical model [16]. An essential rule in validating the study results is to compare the computer model predictions results to experimental data [15]. Disagreements between the computer model predictions and the experiments can be categorized as three distinct factors based on the computer model: (1) Numerical uncertainty (inaccuracy in solving mathematical equations of the problem); (2) Parametric uncertainty (imprecision in model parameters' definition); and (3) Structural uncertainty (inexactness and incompleteness in engineering principles modeling). Calibrating the input parameters of a model without considering structural uncertainty might gain mathematically correct results but physically incorrect solutions [17]. However, the success of model updating procedure depends on experimental test execution. The importance of experimental data acquisition is considerably high not only due to its impact on the accuracy of updated numerical model, but also because of possible real system implementation.

In this paper, the semi-active control of a three-dimensional fixed offshore jacket platform (SPD9 located in the Persian Gulf) is studied over a numerically updated model for the first time to gain the most promising numerical results and to keep the numerical model performance close to the prototype. The experiment is performed using a shake table test and non-contact sensing Laser Doppler Vibrometry (LDV) device and utilizing a scaled hydro-elastic physical model. The updating procedure is carried out by considering both parametric and structural uncertainties within the calculation process. The elastic modulus of the platform members is defined as the calibration parameter to reduce the parametric uncertainties. A mathematical function is also utilized to reduce the structural uncertainties by using Particle Swarm Optimization (PSO) algorithm. Eight MR dampers are placed on the numerically updated model in both X and Y directions and modified Newmark-Beta method base on the instantaneous optimal control algorithm is used to estimate the response of the system. The results show the efficiency of the mentioned methodology by regarding parameter uncertainty for an infrastructural system due to the reduction in disagreement of the experimental data and numerical model in offshore industries. The results also indicate the importance of model uncertainty reduction in improving the accuracy of simulation results in a complex system.

2. Semi-active Control Process

2.1 Experimental Test

In this study, a numerical model updating approach is proposed on a controlled complex structural system. The model is built based on the prototype dimensions by ABS tubes that are welded together using argon arc welding to ensure proper load transfer and the FEM of the platform [18]. To gain 1:100 scale of the prototype, the specifications of the scaled model are considered as listed in Table 1.

Table 1. Properties of the scaled and prototype of the platform model

Properties	Prototype	Model
Height (m)	74	0.74
Low-level dimensions (m)	36×35	0.36×0.35
High-level dimensions (m)	29×16	0.26×0.16
Scale Factor	--	1:100
Material	Steel	ABS (Acrylonitrile Butadiene Styrene)
Platform weight (t)	15500	0.015

The test is implemented using a shake table and a Laser Doppler Vibrometer (LDV) as a non-contact measuring system. The LDV is well established as an efficient, fast, and also cost-effective means of analyzing and measuring device that performs without any surface contact. More details of the experimental test and models are shown in Fig.1 and Table 2.

To carry out the test, the scaled model of the structure is placed on the shake table in X direction for velocity measurement and the LDV is located and adjusted to center the measuring beam in the middle of the jacket deck. The analogue velocity output calibration can be checked employing an appropriate accelerometer in association with a charge amplifier or a standard hand-held calibrator. The calibration procedure is performed based on the optical unit user manual. A random vibration signal is also applied on the scaled model in a frequency range of 1-50Hz with duration of 20 seconds. The test is repeated 3 times to avoid any unintentional errors. The experimental measurement is considered to validate and also update the numerical model. The post-processing procedure is executed using ME'ScopeVES software package based on the captured frequency response functions (FRFs) of the scaled jacket model through the tests.

Fig. 1. Layout of the experimental test using the LDV sensing components and the scaled model.

Table 2. The LDV sensing components and shake table facility specifications

Facilities	Characteristics	Values
Laser Doppler Vibrometry (Optical Unit)	Vibration Velocity	A few μs/m to 425 mm/s
	Vibration Frequency	< 0.1 Hz to 25 kHz
	Working Distance	From 0.4m up to 25m
	Dimensions	75 × 175 × 350mm
	Temperature	+5°C to +35°C
	Relative Humidity	Up to 80%
	Weight	3.7 kg
Shake Table	Rated Frequency Range	0.5 – 1500 Hz
	Size of Table	400 × 400 mm
	Max Displacement	25 mm
	Max Load	70 kg

2.2 Numerical Model Updating

In this study, the mass and stiffness matrices of the jacket finite element (FE) model are gained employing Frame3DD software and modeling the elements and nodes coordinates of the prototype. To consider the uncertainties through the modeling a novel approach is considered. Uncertainties in computer modelling can be categorized into three various factors: (i) numerical uncertainty which is based on inaccuracy in solving method of the equations; (ii) parametric uncertainty which is defined as imprecision in parameters definition of the numerical model; and (iii) structural uncertainty which is due to incompleteness in modeling the engineering principles [19]. Through an iterative process, both structural and parametric uncertainties are considered within the calculation process of this study. In this regard, the calibration parameter for the second factor and a model form error for the third factor are determined as the solution. By proposing a relation between input and output of the modeling (y_{sim}) and the actual physical system and the experimental data ($y_{\exp}$), a formulation can be defined as follows:

$$y_{exp} = \left(y_{sim}(z_i.\theta) + \Psi(z_i)\right) + \varepsilon(z_i) \qquad i = 1.\cdots.n \tag{1}$$

where, $(z.\theta)$ is a relation between the model input and the variables z, θ, $\varepsilon(z_i)$, n, and $\Psi(z_i)$ represent control parameter, calibration variable, the experimental error, the number of experimental tests and the model form error or the discrepancy function, respectively. More details about the mentioned method for updating the numerical model can be found in [15]. The goal of model updating is to reduce the disagreement between the experimental data and numerical modeling using a discrepancy term. In the other hand, the goal is to combine parameter values and discrepancy models to reach the experimental data. Actually, the discrepancy function could be specified as any continuous and differentiable mathematical function, because of trigonometric nature of the experimental data, the model form error is defined as a combination of trigonometric and exponential functions in this paper:

$$\delta(z,\alpha) = \alpha_0 \times e^{(\alpha_1 \times sin(\alpha_2 z+\alpha_3)+\alpha_4 \times cos(\alpha_5 z+\alpha_6))} \tag{2}$$

where, α indicates the nonphysical coefficients. Basically, the aim of the proposed method is to minimize the difference between the simulation and also the experimental data utilizing an objective function and an optimization algorithm:

$$f(\alpha.\theta) = [y_{exp}(z) - \xi(z)]^2 = [y_{exp}(z) - y_{exp}(z.\theta) - \delta(z.\alpha)]^2 \tag{3}$$

$$f(\alpha.\theta) = \sum_{i=1}^{n}[y_{exp}(z_i) - y_{exp}(z_i.\theta) - \delta(z_i.\alpha)]^2 \qquad i = 1.\cdots.n \tag{4}$$

The coefficients introduced by the selected model should be trained with the available experimental data. In this study, the objective function is performed by using the PSO algorithm in which the values of swarm size, and also the social and cognitive acceleration coefficients are chosen as 30, 1.3, and 2.8, respectively. In this paper, acceleration is selected as the output of the experimental and numerical models, time is taken as the control parameter, and modulus of elasticity (E) is chosen as the calibration parameter taken in different ranges based on importance of the elements of the jacket platform. Four distinct groups are defined for the jacket elements consists of the main jacket legs, diagonal, horizontal, and also the internal members. The value of calibration parameter for each group is listed in Table 3. Unlike other structural systems, in offshore jacket platforms, the main legs are the most important structural members, then bracing, the horizontal, and finally the internal members can be considered as the most to less important members. Two main leg and bracing members have the highest effects on the first five modes (natural frequencies), while the horizontal member includes the lowest impact on modes. The final objective function of the optimization algorithm is as follows:

$$f = \sum_{i=1}^{n}[\ddot{x}_{exp}(t_i) - \ddot{x}_{sim}(t_i.E_1.E_2.E_3.E_4) - \delta(t_i.\alpha_0.\alpha_1.\alpha_2.\alpha_3.\alpha_4.\alpha_5.\alpha_6)]^2 \qquad i = 1.\cdots.n \quad (5)$$

Table 3. Group of elements lower and upper bounds (initial value is based on steel modulus of elasticity)

Bounds	Main Legs	Horizontal Elements	Diagonal Elements	Internal Elements
Lower bound	194000 MPa (-3%)	192000 MPa (-4%)	192000 MPa (-4%)	190000 MPa (-5%)
Upper bound	206000 MPa (+3%)	208000 MPa (+4%)	208000 MPa (+4%)	210000 MPa (+5%)

More details of the proposed updating algorithm are presented in Table 4. Natural frequencies of the experimental, numerical, and updated models are also presented in Table 5.

Table 4. Algorithm of model updating procedure

	Algorithm of Proposed Updating Strategy
	A) Considering an optimization algorithm. B) Defining a discrepancy model, Eq. 4. C) Defining an objective function: Eq. 5.
1:	Assume: $t_i.E_1.E_2.E_3.E_4.\alpha_0.\alpha_1.\alpha_2.\alpha_3.\alpha_4.\alpha_5,\alpha_6$;
2:	Put the assumed values of *E* into the Frame3DD input File;
2:	Compute $M_d.K_d$ as the Mass and Stiffness Matrices through Frame3DD;
	Load $\ddot{x}_{exp}$,$M_d.K_d$;
3:	Compute the $\ddot{x}_{sim}$ By solving the equation of motion using the same scaled experimental force;
4:	Compute f as the objective function considering assumed values of α for the discrepancy function;
5:	Is the objective function satisfied? Yes, Go to next Step or No go to Step 1;
6:	Stop.

Table 5. Natural frequencies of experimental, numerical, and updated models (Hz)

Natural Frequencies	Experimental Model (Scaled Model)	Numerical Model	Updated Numerical Model without Discrepancy Term	Updated Numerical Model with the Discrepancy Term
Mode 1	11.3	13.72	13.12	11.79
Mode 2	36.6	35.57	35.77	36.24
Mode 3	68	69.21	68.64	68.13

According to the results as listed in Table 5, the updated models is fitted almost poorly by utilizing the optimization process. However, as the proposed discrepancy function is defined within the updating process, higher fitness tendency could be observed. To be more specific, employing a discrepancy function or a model form error term within the numerical model updating procedure is strongly recommended. In this study, to show the importance of numerical model updating before applying the semi-active system, both numerical models (not updated) and updated model with discrepancy are compared under El Centro earthquake ground acceleration as represented in Fig. 2. Accordingly, there are obvious differences, anti-phase peaks, and amplitudes between the response of the numerical model before and after updating under an earthquake force. It is seen that achieving trustworthy numerical results not only requires a valid experimental test but also needs an efficient model updating approach before any further investigations. Displacement RMS of both numerical models are listed in Table 6.

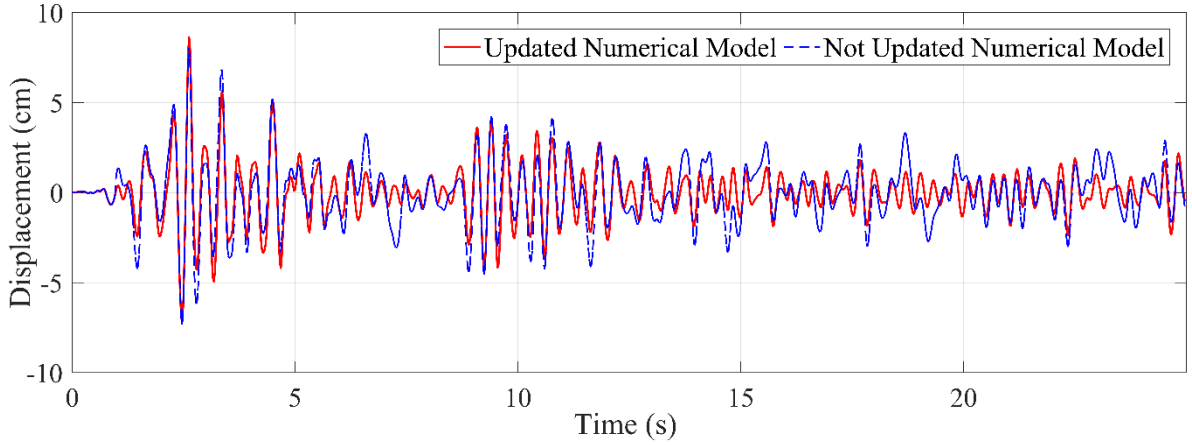

Fig. 2. Updated and Not Updated Numerical Models Comparison under El Centro Earthquake

Table 6. Displacement RMS of Updated and not Updated Numerical Models under El Centro Earthquake

Index	Numerical Model	Updated Numerical Model with the Discrepancy Term	Difference (%)
RMS	0.876	1.32	34

As seen in Table 6, the differences between the numerical models with and without updating is about 34 percent which is much higher than acceptable range. The result of Table 5 is a confirmation of model updating requirements.

2.3 Modelling MR Damper

MR dampers are one of the most promising semi-active control devices in civil engineering applications [10]. General equation of motion of the jacket platform equipped with MR damper can be expressed as follows:

$$[M^*]\cdot\{\ddot{x}\}+[C^*]\cdot\{\dot{x}\}+[K]\cdot\{x\}=\{F_W \; or \; F_E\}+[L]\cdot\{F_{MR}\} \quad (6)$$

where, F_W and F_E are n-dimensional wave loading vector and ground motion force, respectively; $\{\ddot{x}\}$, $\{\dot{x}\}$, and $\{x\}$ are vectors of acceleration, velocity and displacement, all with $n \times 1$ dimensions, respectively; $[M^*]$ and $[C^*]$ are mass and damping matrices of the jacket system considering added mass and damping, respectively, which are discussed in following; $[K]$, L and $\{F_{MR}\}$ are the jacket stiffness matrix, the matrix denoting the location of controllers, and the MR dampers force vector including f_d as each MR dampers control force, respectively. An illustration of modified Bouc-Wen model is shown in Fig. 3.

$$f_d = c_1 e + k_1(u_{MR} - x_0) \quad (7)$$

where, the evolutionary variable is known as *y* and also the variable *e* is coupled equations as follows:

$$\dot{y} = -\gamma|v_{MR}-\dot{e}|(y)|y|^{(n-1)} - \beta(v_{MR}-\dot{e})|y|^{(n)} + A_{MR}(v_{MR}-\dot{e}) \quad (8)$$

$$\dot{e} = \left\{\frac{1}{c_0+c_1}\right\}\{\sigma_0 y + c_0 v_{MR} + k_0(v_{MR}-e)\} \quad (9)$$

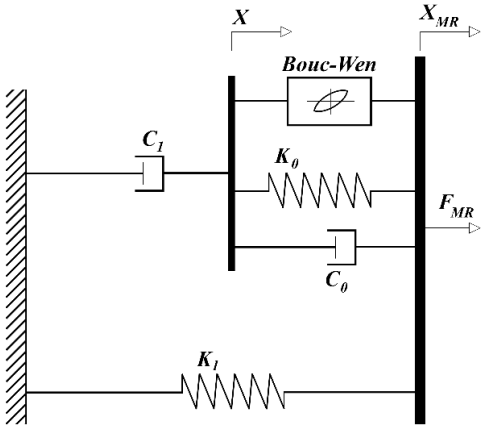

Fig. 3. Modified Bouc-Wen model

where v_{MR}, u_{MR}, k_0, and k_1 are relative velocity and displacement between connected joints in jacket members, control damper force in large velocities and accumulator stiffness respectively. The hysteresis loops shape depends on parameters A_{MR}, γ, and β. Variables c_0, c_1, and σ_0 are large velocities viscous damping coefficient, low velocities viscous damping coefficient and also evolutionary coefficient, respectively, which can be gained using the following equations based on the command voltage *u*:

$$c_0 = c_{0a} + c_{0b}u \quad (10)$$

$$c_1 = c_{1a} + c_{1b}u \quad (11)$$

$$\sigma_0 = \sigma_{0a} + \sigma_{0b}u \quad (12)$$

where, variable u is obtained within first order filter as:

$$\dot{u} = -\mu(u - v) \quad (13)$$

where variable v is control voltage, which can be determined using a control algorithm. Based on specification of MR damper and semi-active control method, choosing an appropriate algorithm not only increases the semi-active control system performance but also decreases the structure response. In this paper, the Lyapunov algorithm [8] is used as follows:

$$v = v_{max}H(-Z^T P_L B f_d) \quad (14.A)$$

where $[P_L]$ is real, symmetric, positive definite matrix, can be calculated through:

$$[A^T][P_L] + [P_L][A] = -[Q_P] \quad (14.B)$$

$$\dot{Z} = AZ + BF_d + E\ddot{x}_g \quad (14.C)$$

$$Z = \begin{bmatrix} x \\ \dot{x} \end{bmatrix}; B = \begin{bmatrix} 0 \\ -M^{-1}D \end{bmatrix}; A = \begin{bmatrix} 0 & 1 \\ M^{-1}D & -M^{-1}C \end{bmatrix}; E = \begin{bmatrix} 0 \\ r \end{bmatrix} \quad (14.D)$$

where, $H(\cdot)$ is Heaviside step function. The voltage, which should be applied to the damper, must be taken as v_{max} if the step function is higher than zero and in other cases, the command voltage must be set to zero. Variables Z, $[B]$, $[A]$, $[Q_P]$ are the state space vector with $2n \times 1$ dimensions, a state space parameter matrix, system matrix with $2n \times 2n$ dimensions, and a matrix of unity, respectively. In this paper, MR dampers are modelled within the braces (not to be replaced with braces) in upper two structural levels. Location of eight mentioned dampers are shown in Fig. 4 for both X and Y directions.

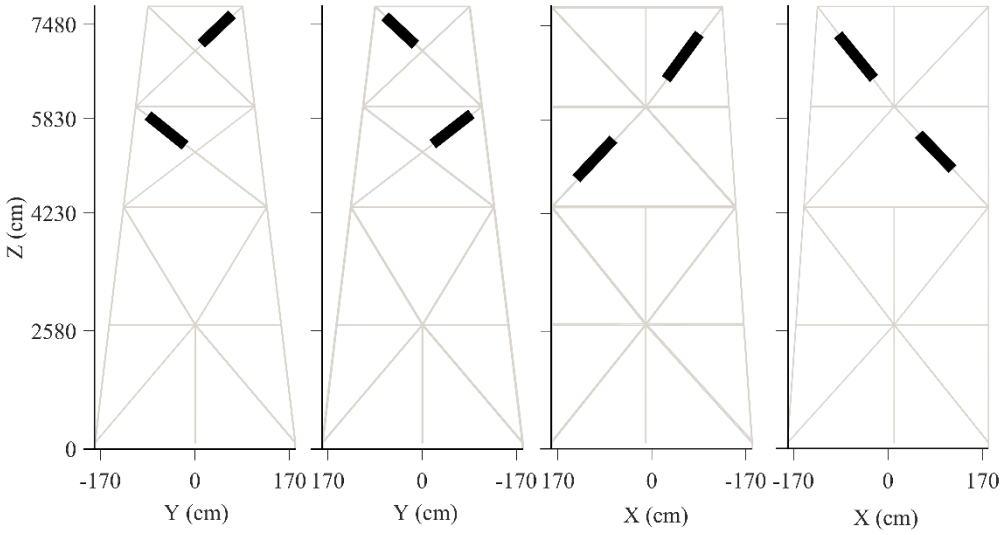

Fig. 4. Location of MR dampers: (A) X Direction; (B) Y Direction

Because of the strong nonlinear hysteretic behavior of MR dampers, the instantaneous optimal control algorithm based on Newmark's integration is used mode detail of which is available in the literature [10, 20].

2.4 Environmental Loads

The performance of the updated system is studied under environmental loads in this paper. Based on Eq. 6, the system mass and damping matrices considering added mass and damping can be derived as follows:

$$[\bar{M}] = [M] + \rho_w(C_M - 1)V \quad (15)$$

$$[\bar{C}] = [C] + \frac{1}{2}\sqrt{\frac{8}{\pi}}\rho_w C_D A \sigma_{vr} \quad (16)$$

where $[M]$ and $[C]$ are the jacket mass and damping matrices, respectively; ρ_w, V, A, C_D, C_M, and σ_{vr} are the mass density of water, displaced volume of the member, projected area normal to the member axis, drag coefficient, inertia coefficient, and the value of root mean squares of the relative velocity between the jacket and water particles, respectively. It should be noted that the Rayleigh's technique is used for the jacket damping matrix. The hydrodynamic force (chosen as wave) is calculated based on a wave theory. Wave induced forces can be calculated using the Morison Equation for a cylinder type structure as follows [21]:

$$F_W = \rho_w V C_M \ddot{q}_n + \frac{1}{2}\rho_w C_D A|\dot{q}_n - \dot{x}_n|(\dot{q}_n - \dot{x}_n) \quad (17)$$

$$F_W = \rho_w V C_M \ddot{q}_n + \frac{1}{2}\sqrt{\frac{8}{\pi}}\rho_w C_D A \sigma_{vr}(\dot{q}_n - \dot{x}_n) \quad (18)$$

where F_W is the wave force per unit length of the member; $\ddot{q}_n$, $\dot{q}_n$, $\dot{x}_n$, and $(\dot{q}_n - \dot{x}_n)$ indicate the acceleration of the fluid, velocity of the fluid, the absolute velocity, and the relative water velocity at joint *n*, respectively. In this paper, Morison equation (linearized form) is employed and the main parameters of wave height and period, are taken based on sea state of the Persian Gulf with 100 years of return period (see Table 7) [22]. The velocities and accelerations of the water particle are evaluated utilizing the Stokes second order wave theory [23]. Characteristics of the hydrodynamic force are listed in Table 8.

Table 7. Persian Gulf sea state characteristics [22]

Return period (year)	Wave height H_s (m)	Peak period T_p (s)
10	4.15	5.59
20	4.67	6.35
50	5.33	6.77
100	5.83	7.10

Table 8. Specification of hydrodynamic force

Specification	Values
Wave return period (year)	100
Wave heights (m)	5.83
Wave periods (s)	7.10
Water depth (m)	69.5
C_d	0.7
C_m	2

3. Results and discussion

In this study, a semi-active control of an offshore steel jacket platform is performed based on a truly updated numerical model. In this regard, the PSO algorithm is performed by 100 runs with detailed specification of swarm size of 30 and 150 iterations. The calibrated values of elastic modulus for all four groups and the value of the best fitness function (sum of squared errors) are listed in Table 9. Updated numerical model is used to investigate the structural response and semi active control of the jacket employing MR damper with 200kN capacity. The control force of the dampers is calculated using modified Bouc-Wen method. Time history response of one of the top nodes of the structure (Node 1) is illustrated in Fig. 5 using the same but scaled sinus force which is applied to the experimental model. The calculated acceleration in finite element model (obtained by the sinus force) is compared to the recorded acceleration of the experiment for updating the numerical model. For a better explanation, the scaled force of the experiment is applied into numerical model and used for updating the numerical model. In Fig. 5, two cases are compared in each figure as un-controlled structure (Uncontrolled) and semi-active controlled structure (Controlled). It is seen that using MR dampers effect on whole structural response to decrease. Fig. 5.B represents the control force of the damper as an important factor both in semi-active control process and MR damper device because of damper force limitations (MR damper can apply limited forces to the structure according to its specification).

Table 9. Calibrated values of Elastic Modulus for four groups of elements and related SSE

Values	Main Legs	Horizontal Elements	Diagonal Elements	Internal Elements
Optimized E (MPa)	200830	202500	196230	199410
SSE (g^2)	0.89×10^{-8}	0.89×10^{-8}	0.89×10^{-8}	0.89×10^{-8}

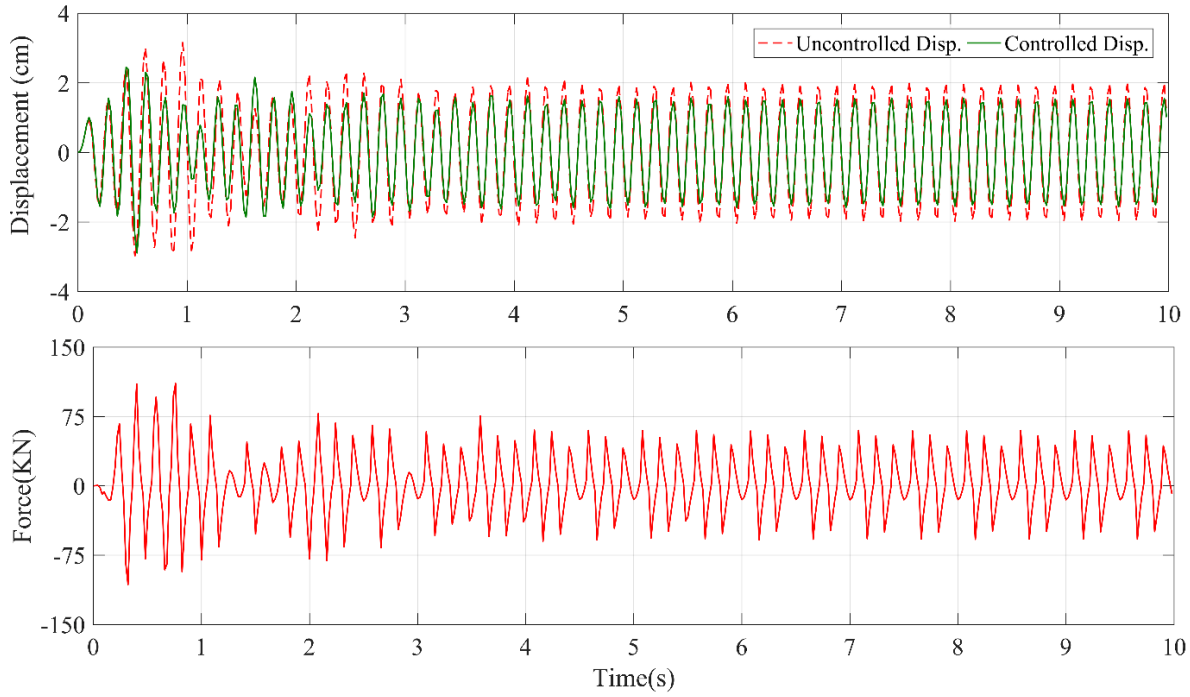

Fig. 5. Time History of Displacement and Control Force of the Jacket Platform under Sinus Force

Efficiency of the dampers are also investigated under wave and earthquake loads in this manuscript. A wave with 100 years of return period is assumed based on characteristics of Table 7 and 8. Time history of top node displacement is demonstrated under wave in Fig. 6 for uncontrolled and controlled systems. The whole system response is decreased using MR damper in both amplitude of the response and the number of the peak points which results in lower vibration in the whole system and the system lifespan improvement.

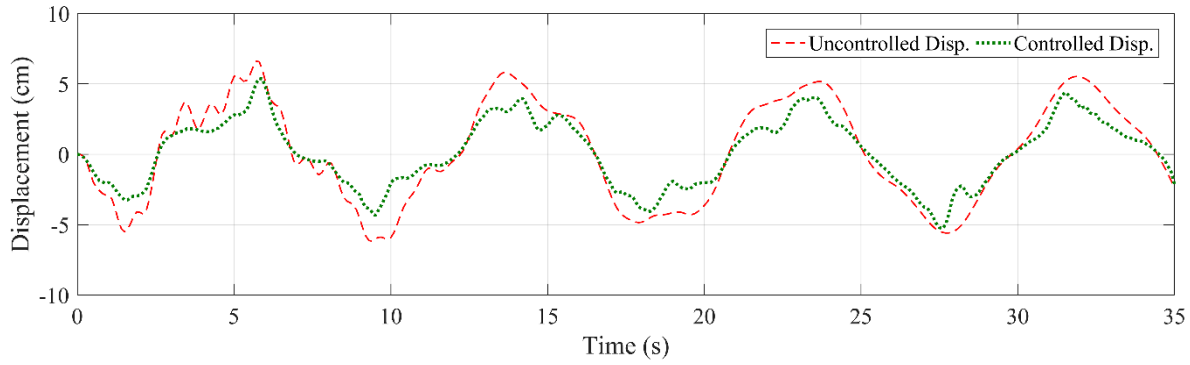

Fig. 6. Time History of Top Node Displacement under Regular Wave Load

The structural response of the jacket platform is also investigated under three major earthquake records. Proposed records are chosen as near field unidirectional ground motion records such as El-Centro, 1940, Kobe, 1995, San Fernando, 1971. Time history of top node displacement under three proposed earthquake excitations are also shown in Fig. 7. The mentioned controlled strategy results in lower vibration and the whole response reduction. The structural vibration is not only decreased through lower amplitudes but also it is reduced within lower response frequencies. Presented structural response of the jacket platform in Fig. 7 proves that using semi-active MR damper in offshore jacket platforms is an appropriate choice. Hysteresis behavior of MR damper under earthquake records is shown in Fig. 8. Nonlinear behavior of MR damper is also illustrated in hysteresis loops of Fig. 8. A summary of peak displacement and control force of top node of the jacket are listed in Table 10 for comparison.

Table 10. Summary of peak top node displacement and controlled force results under earthquake

Earthquakes	Displacement (cm)		Control force (kN)
	Uncontrolled	Controlled	
El-Centro	8.8	3.69	148
Kobe	9.8	4.82	91
San Fernando	5.8	3.71	84

4. Conclusion

Semi-active control of an offshore steel jacket platform is investigated over a numerically updated model using non-contact experimental data. The experiment is implemented using a shake table test, a non-contact LDV device, and a scaled hydro-elastic physical model of the jacket platform. The simultaneous reduction of structural and calibration parameters, which is specified as the baseline of the semi-active control system through as optimization framework, is investigated in details in this paper. The results and limitation of the study can be summarized as follows:

- The numerical model of the investigated offshore platform is updated successfully using non-contact measurements. Accordingly, utilizing an LDV sensing components is recommended because of both no direct contact requirements and also great sensitivity of non-contact sensing technology.
- Numerical updating is performed not only to achieve the most promising numerical results but also to keep the results as much close to the actual physical model behavior as possible. Therefore, updating the numerical model based on experimental data before taking a structural control strategy into account is strongly recommended.
- The results show the efficiency of the updating methodology by regarding parameter uncertainty for an infrastructural system due to the reduction in disagreement of the experimental data and numerical model in offshore industries. Based on the model updating results, which indicates the capability of the introduced model updating procedure, considering such methodology within the calculation is of great importance mostly before any further investigation on the numerical model.
- Considered trigonometric-based function, which is used for the first time as a discrepancy function in an offshore infrastructure, performed acceptably as discussed in the results.
- The proposed control devices result in lower vibration. The structural vibration is not only decreased through lower amplitudes but also it is reduced within lower response frequencies under both wave and earthquake loads. Simply put, the whole system response is decreased using MR damper in both amplitude of the response and the number of the peak points which results in lower vibration in the whole system and the system lifespan improvement.
- Definitely, it is not possible to assess all aspects of a research through a single study. Therefore, other problems are remained unsolved particularly in relation to practical cases which must be considered as the topics of the futures studies.

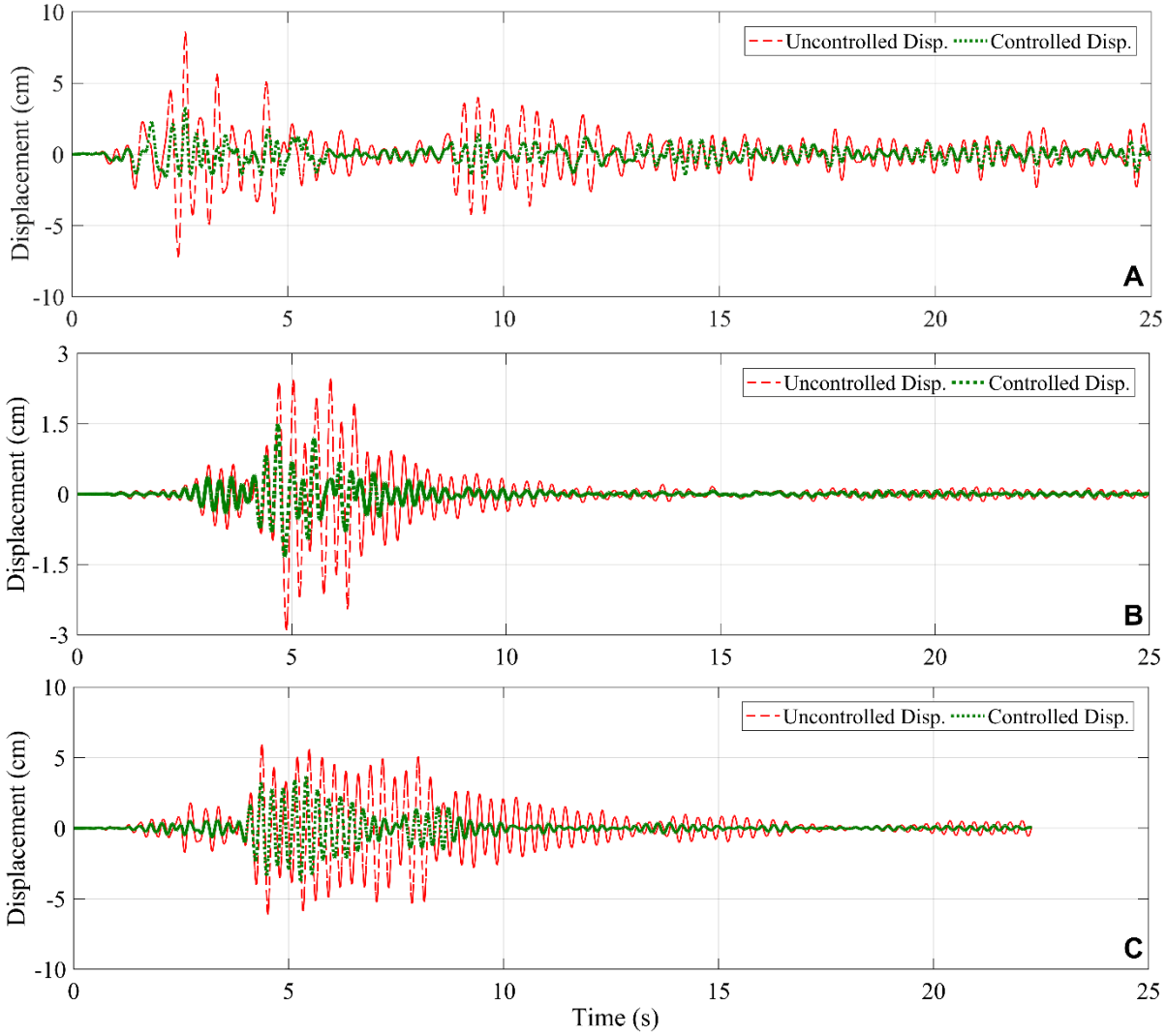

Fig. 7. Time History of Top Node Displacement under Earthquake Excitations: (A) El-Centro, (B) Kobe, (C)

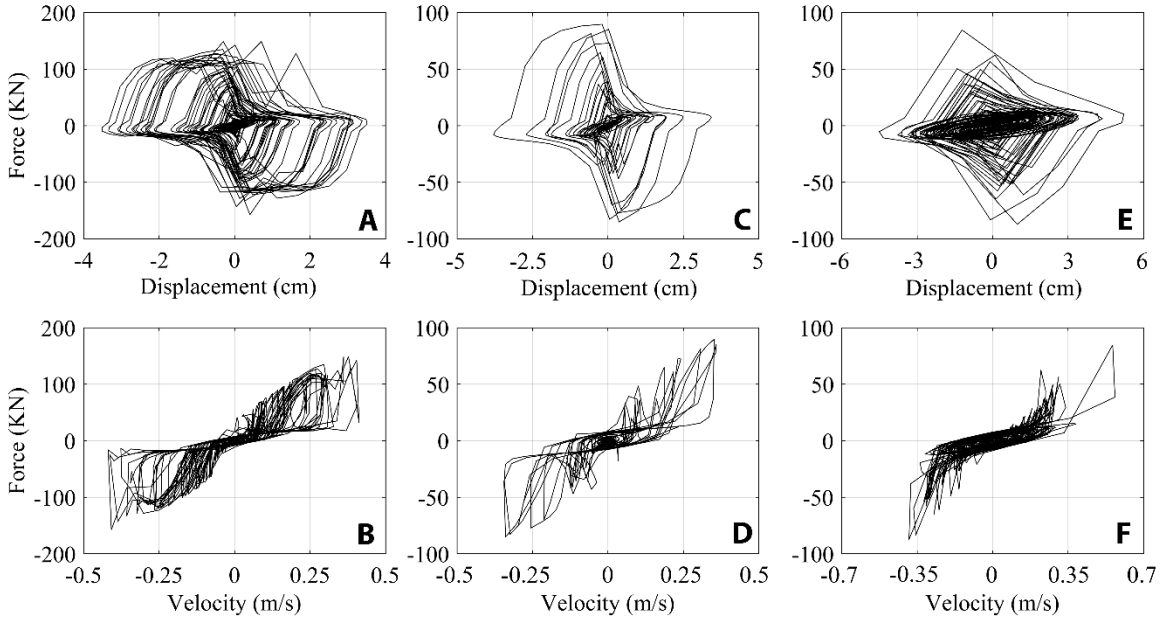

Fig. 8. Hysteresis behavior of MR damper under earthquake:
(A, B) El-Centro; (C, D) Kobe; (C, D) San Fernando

References

[1] Kandasamya R., Cuia F., Townsend N., Foo C.C., Guo J., Shenoi K., Xiong Y. (2016). A review of vibration control methods for marine offshore structures. Ocean Engineering. 127: 279–297.

[2] Som A., Das D. (2018). Seismic vibration control of offshore jacket platforms using decentralized

sliding mode algorithm. Ocean Engineering. 152:377–390.

[3] Fisco N.R., Adeli H. (2011). Smart structures: Part I - Active and semiactive control, Scientia Iranica, 18(3): 275-284.

[4] Housner G.W., Bergman L.A., Gaughey T.K., Chassiakos A.G., Claus R.O., Masri S.F., Skelton R.E., Soong T.T., Spencer B.F., and Yao J. (1997). Structural control: past, present, and future, Engineering Mechanics. 123(9): 897-971.

[5] Hokmabady H., Mohammadyzadeh S., Mojtahedi A., (2019). Suppressing structural vibration of a jacket-type platform employing a novel Magneto-Rheological Tuned Liquid Column Gas Damper (MR-TLCGD). Ocean Engineering. 180:60–70.

[6] Chen D., Huang S., Huang C., Ouyang F. (2021). Passive control of jacket–type offshore wind turbine vibrations by single and multiple tuned mass dampers, Marine Structures, 77:102938.

[7] Ghadimi, B., Taghikhani T. (2021). Dynamic response assessment of an offshore jacket platform with semi-active fuzzy-based controller: A case study, Ocean Engineering, 238:109747.

[8] Dyke S.J., Spencer B.F., Sain M.K., Carlson J.D. (1997). Phenomenological model for magnetorheological dampers, Engineering Mechanics, 123(3):230-238.

[9] Yoshioka H., Ramallo J.C., Spencer B.F. (2002). Smart base isolation strategies employing magnetorheological dampers, Engineering Mechanics. 128(5): 540-551.

[10] Katebi J., MohammadyZadeh S. (2016). Time delay study for semi-active control of coupled adjacent structures using MR damper. Structural Engineering and Mechanics. 58(6):1127-1143.

[11] Sarrafan A., Zareh S.H., Khayyat A.A., Zabihollah A. (2012). Neuro-fuzzy control strategy for an offshore steel jacket platform subjected to wave-induced forces using magnetorheological dampers. Mechanical Science Technology. 26(4): 1179–1196.

[12] Chunyan J., Menglu C., Shanshan L. (2010). Vibration control of jacket platforms with magnetorheological damper and experimental validation. High Technology Letters, 16(2):189–193.

[13] Bitner-Gregersen E.M., Ewans K.C., Johnson M.C. (2014). Some uncertainties associated with wind and wave description and their importance for engineering applications. Ocean Engineering. 86:11–25.

[14] Negro V., López-Gutiérrez J., Esteban M.D., Matutano C. (2014). Uncertainties in the design of support structures and foundations for offshore wind turbines, Renewable Energy. 63:125–132.

[15] Hokmabady H., Mojtahedi A., Lotfollahi Yaghin M.A., Farajpour I. (2019). Calibration and Bias-Correction of the Steel Offshore Jacket Platform Models Using Experimental Data, Waterway, Port Coastal and Ocean Engineering. 145(3):04019008.

[16] Wu J.R., Li Q.S. (2006). Structural parameter identification and damage detection for a steel structure using a two-stage finite element model updating method, Constructional Steel Research. 62: 231–239.

[17] Hokmabady H., Mohammadyzadeh S., Mojtahedi A. (2020). Uncertainty analysis of an offshore jacket-type platform using a developed numerical model updating technique, Ocean Engineering. 211:107608.

[18] Mojtahedi A., Hokmabady H., Yaghubzadeh A., Mohammadyzadeh S. (2020). An improved model reduction-modal based method for model updating and health monitoring of an offshore jacket-type platform, Ocean Engineering. 209:107495.

[19] Christie M.A., Glimm J., Grove J.W., Higdon D.M., Sharp D.H., Wood-Schultz M.M. (2005). Error analysis and simulations of complex phenomena. Los Alamos Science, 29:6–25.

[20] Joghataie A., Mohebbi M. (2012). Optimal control of nonlinear frames by Newmark and distributed genetic algorithms. Tall and Special Buildings. 21(2):77-95.

[21] Wilson J.F. (2003). Dynamics of offshore structures, John Wiley & Sons Inc. Hoboken, New Jersey, USA. pp. 28-29.

[22] Dastan M.A., Mohajernassab S., Seif M.S., Tabeshpour M.R., Mehdigholi H. (2014). Assessment of offshore structures under extreme wave conditions by Modified Endurance Wave Analysis, Marine Structures. 39:50-69.

[23] Chakrabarti S.K. (2005). Handbook of offshore engineering. Elsevier, Plainfield, Illinois, USA, pp. 91-93.